Journal of Applied Polymer Science

Tung Oil-Based Thermosetting Polymers for Self-Healing Applications

Peter R. Hondred,[1] Leo Salat,[1] Josh Mangler,[2] Michael R. Kessler[1,3]
[1]Department of Materials Science and Engineering, Iowa State University, Ames, Iowa 50011
[2]Science Department, Dallas Center-Grimes, Iowa Public School, Iowa
[3]School of Mechanical and Materials Engineering, Washington State University, Pullman Washington 99164
Correspondence to: Michael R. Kessler (E-mail: MichaelR.Kessler@wsu.edu).

ABSTRACT: Several bio-renewable thermosetting polymers were successfully prepared from tung oil through cationic polymerization for the use as the healing agent in self-healing microencapsulated applications. The tung oil triglyceride was blended with its methyl ester, which was produced by saponification followed by esterification. The changes in storage modulus, loss modulus, and glass transition temperature as functions of the methyl ester content were measured using dynamic mechanical analysis. In addition, the fraction of cross-linked material in the polymer was calculated by Soxhlet extraction, while proton nuclear magnetic resonance, Fourier transform infrared spectroscopy and TEM were used to investigate the structure of the copolymer networks. The thermal stability of the thermosets as a function of their methyl ester blend contents was determined by thermogravimetric analysis. Finally, the adhesive properties of the thermosets were studied using compressive lap shear and the fracture surfaces were analyzed using SEM. © 2014 Wiley Periodicals, Inc. J. Appl. Polym. Sci. **2014**, *131*, 40406.

KEYWORDS: biomaterials; biopolymers and renewable polymers; thermosets

Received 23 September 2013; accepted 9 January 2014
DOI: 10.1002/app.40406

INTRODUCTION

Since the late 1950s, the field of polymers and composites has seen unparalleled growth in this country and world-wide.[1] With this development came the realization that the fossil feedstocks used in the manufacture of traditional polymers are being depleted at a rapid pace.[2] Consequently, petroleum shortages, increasing prices, and environmental concerns are a threat to sustained growth and economic viability of traditional plastics in the industry. Thermosetting polymeric materials must overcome additional environmental concerns, because a majority of petroleum-based materials are non-biodegradable.[3,4] To allow further expansion of polymers and composites in a variety of applications, new polymers derived from renewable feedstocks must be developed for the benefit of economy and environment.

Limited research has been performed on the development of high molecular weight polymers from fats and oils.[5,6] One such renewable feedstock avenue under investigation is vegetable oils such as corn, soybean, peanut, canola, tung, and castor oil. Larock et al. showed that the unsaturation in the fatty acid chains can be utilized to produce crosslinking thermosetting polymers.[7–11] These polymers exhibit good thermomechanical properties as well as excellent dampening properties.[10,12] In addition, these renewable feedstocks provide varying degrees of unsaturation depending on the oil chosen, so customization for individual polymer applications is readily available.

Targeted variations in fatty acid chain composition allows for the creation of a wide range of material properties. In this work, the thermo-mechanical properties of bulk polymers derived from vegetable oil are investigated as potential healing agents for self-healing applications—specifically crack filling healing.[13] Although there are multiple methods to approach crack filling healing, all methods rely on the fact that the healing agent polymerizes in the apparent crack and solidifies, creating an adhesive bond to arrest further crack development and maintain the plastic's mechanical integrity [13]. Figure 1 illustrates the microencapsulation strategy for crack filling healing.

The initial work by Larock et al. indicated that these vegetable oil thermosets present potential for self-healing applications. An effective healing agent must meet the following requirements:

1. Materials must exhibit low viscosity, volatility, and good wettability properties.
2. Minimal diffusion through matrix and fast reaction kinetics.
3. Good adhesive strength and mechanical properties of resulting polymer.

This work utilized a cationic polymerization process for tung oil, a reactive vegetable oil, and blended comonomers to modify viscosity, wettability, reaction kinetics, adhesive strength, and mechanical properties. Previous work showed that comonomers such as styrene and divinylbenzene reduced the nonuniformity

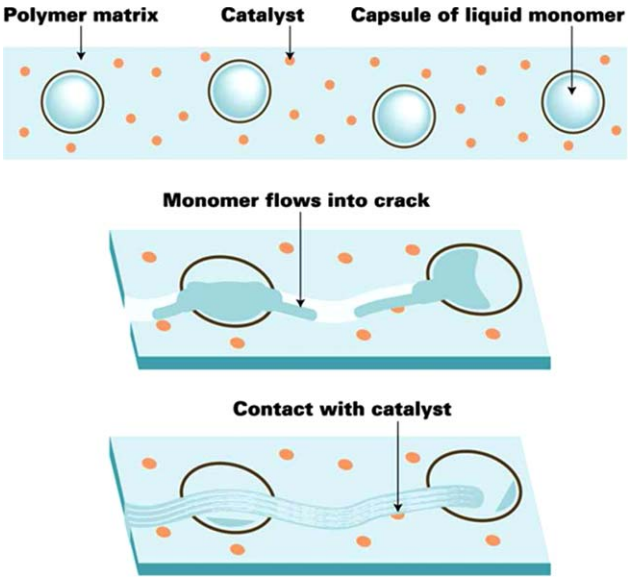

Figure 1. Microencapsulation technique with liquid encapsulated monomer and an imbedded solid catalyst. Reprinted with permission of Ref. 1. [Color figure can be viewed in the online issue, which is available at wileyonlinelibrary.com.]

of the crosslinking structure and improved the mechanical integrity of the resulting polymers.[14,15] In addition, methyl ester derivatives of tung oil were blended with tung oil triglyceride in order to modify the crosslink density of the thermosetting network. The primary focus of this article is on the effect of methyl ester on both the properties of the monomers as well as the properties of the thermosetting polymer. It is anticipated to utilize varying compositions to accommodate the composite material into which these healing agents will be imbedded.

While recent developments in high modulus bioplastics produced materials whose properties resembled those of unsaturated polyesters, current work on self-healing materials utilizes almost exclusively petroleum-based materials. Polymers produced utilizing the unsaturation in vegetable oils are the first step in providing viable material alternatives in the self-healing field.

MATERIALS

In this work, tung oil, also known as China wood oil, was used. While the common China wood oil for wood finishing, available from any hardware or carpentry store, is suitable for the polymerization process, here we used tung oil purchased from Sigma–Aldrich for ease of supply stability and material consistency. Varying amounts of tung oil methyl ester produced by saponification and esterification of the tung oil itself were blended with the tung oil.Styrene and divinylbenzene were also purchased from Sigma–Aldrich. Synthesis grade boron trifluoride diethyl etherate ($BF_3{\cdot}OEt_2$) purchased from Sigma–Aldrich was used as initiator for the cationic polymerization process. The initiator was mixed with SG1100 (a soybean oil methyl ester purchased from SoyGold, Omaha, NE) to enhance solubility. Figures 2 and 3 show the structures of tung oil and its corresponding methyl ester, respectively. Tung oil triglycerides are

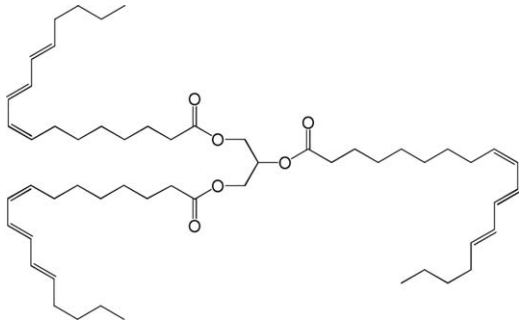

Figure 2. Tung oil triglyceride.

composed of several different fatty acids. The figures show triglycerides and methyl esters based on the dominant fatty acid, α-eleostearic acid, which comprises 82% of the fatty acid chains. This fatty acid is identified by three conjugated double bonds. The remaining 18% fatty acids exhibit less reactive levels of unsaturation.

Synthesis

The following polymerization process was employed unless explicitly stated otherwise: First, the monomers were hand-mixed at room temperature in their desired amounts according to Table I. The initiator, boron trifluoride diethyl etherate, and its solubility enhancer were hand-mixed at room temperature separately because boron trifluoride diethyl etherate is moisture sensitive. Therefore, initiator and enhancer were mixed in an inert environment, i.e., in a glove box, sealed in a vial, and removed by syringe as required for the reaction.

The monomer mixture was placed on a stir plate inside an ice bath. Once the monomers had cooled in the ice bath down to 0°C, a stir bar was placed in the mixture, and the initiator was added via syringe while constantly mixing. The sample was allowed to mix for 10 s and then removed from the ice bath to solidify. Within a matter of seconds, the sample solidified in the vial. Samples were postcured in the oven for 1 h at 120°C to complete the polymerization process. The reaction was a cationic process (shown in Figure 4), in which the initiator, boron trifluoride diethyl etherate, reacted with the unsaturation sites in the monomers. Different compositions for these thermosetting polymers are listed in Table I.

The changes in material properties as a function of methyl ester blend were investigated. Tung oil was removed and replaced with its respective methyl ester derivative to change the composition of the polymer. Tung oil methyl ester monomer for synthesis was created by saponification and esterification. For

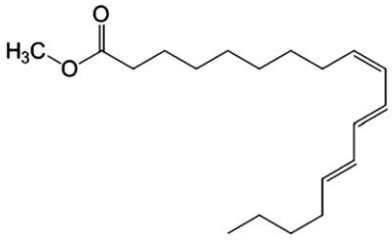

Figure 3. Tung oil methyl ester.

Table I. Variation in Composition of Thermosetting Biopolymers in wt %

	Tung oil triglyceride	Tung oil methyl ester	Styrene	Divinylbenzene	Initiator
47.0% Tung oil	47.0%	0%	30%	15%	8%
42.3% Tung oil	42.3%	4.7%	30%	15%	8%
37.6% Tung oil	37.6%	9.4%	30%	15%	8%
32.9% Tung oil	32.9%	14.1%	30%	15%	8%
28.2% Tung oil	28.2%	18.8%	30%	15%	8%

The initiator was comprised of 5% SoyGold and 3% $BF_3{\cdot}OEt_2$.

saponification (the cleaving of the fatty acid chains) 100 g of tung oil and 200 cm^3 of NaOH (10%) solution were mixed, heated for 2 h, and stirred until emulsified. Once emulsified, 300 cm^3 of water was added and the mixture was heated for an additional 30 min. Once the solution became translucent, indicating complete saponification, it was poured into 650 cm^3 of hot water with 100 cm^3 of 20% hydrochloric acid and was heated for an additional 20 min until it was transparent. Cooling in an ice bath under constant stirring, the solution solidified into small agglomerations. These agglomerations of fatty acid were washed with water to remove excess salts. Finally, the fatty acid agglomerations required further drying to remove any residual water trapped during the solidification in the cooling down period, which was accomplished by heating above melt temperature and extracting the phase separated water. Once the fatty acid was obtained, it was converted into methyl ester by esterification.

For esterification, 50 g tung oil fatty acid was dissolved in 500 mL of methanol and placed on a hot plate to facilitate dissolution. Once dissolved a catalytic amount of sulfuric acid was added under constant mixing. The solution was distilled for 2 h and the reaction was monitored for completion using thin layer chromatography. Once the fatty acid was converted into methyl ester, the solvent was removed utilizing a rotary evaporator. Subsequently, an aqueous workup was used to wash out the acid with water and ethyl ether anhydrous. Mixing with magnesium sulfate for 15 min removed any residual water. Finally, the magnesium sulfate was removed by filtering and washing with ethyl ether anhydrous and tung oil methyl ester was isolated by rotary evaporation. The purity of the sample was verified through NMR. The process of saponification and esterification is shown in Figure 5.

RESULTS AND DISCUSSION

Dynamic mechanical analysis was performed on samples with the five different compositions described in Table I. The DMA results are shown in Figures 6–8. All tests were run at a fixed heating rate of 10°C min^{-1}. Figure 6 shows the change in storage modulus as a result of change in monomer ratios. As tung oil methyl ester was substituted for tung oil triglyceride, the storage modulus in both the glassy and rubbery regions decreased. These data were used to calculate the crosslink

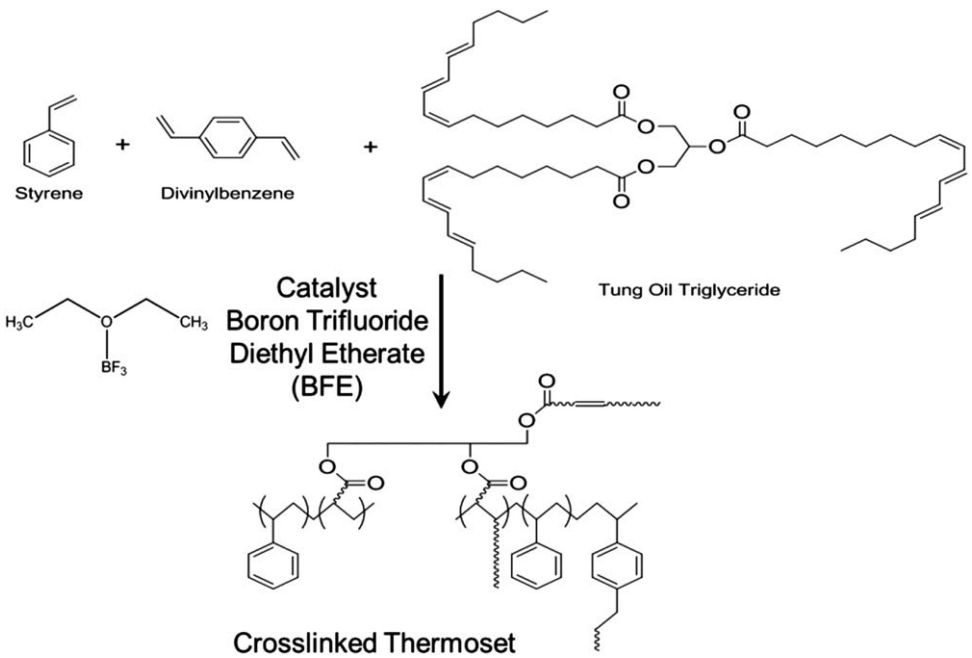

Figure 4. Cationic polymerization of tung oil, styrene, and divinylbenzene.

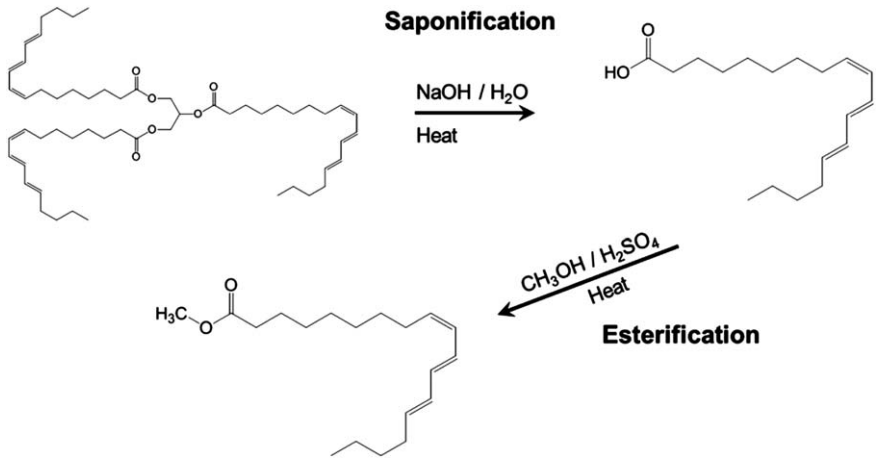

Figure 5. Saponification and esterification of tung oil to obtain the methyl ester derivative.

density of the thermoset. Crosslink density was determined by calculating the polymer's molecular weight between the crosslinking points. This molecular weight value is calculated from the rubbery plateau, secondary (lower) region in the temperature values of 100–150°C, of the storage modulus found in Figure 6.

The molecular weight of the chain between crosslink sites, M_c, was utilized to compare the crosslink density of the different polymer compositions, because as the molecular weight between the crosslinks increased, the crosslink density decreased.[16] The following equation is used to calculate the molecular weight between crosslinks:

$$M_c = \frac{3qdRT}{E'_{T_g+50K}} \quad (1)$$

where E'_{T_g+50K} represents the storage modulus at 50K above the glass transition temperature determined by the maximum peak value of tan δ in Figure 7. The variables q, d, R, and T are the front factor, density of the fully cured material at room temperature, gas constant, and temperature at 50K above the glass transition temperature, respectively [15]. In this case, q is 1 since this is standard for the majority of polymers.[17] Table II provides the crosslink density for the different compositions of tung oil derived thermosets. As expected, the crosslink density decreased, as indicated by the increasing molecular weight between crosslinks, with increasing methyl ester because of fewer available glycerol bonds in the triglyceride.

Figure 7 provides the phase angle, tan δ, for the different compositions of tung oil derived polymers. For each composition, the maximum value of tan δ represents the glass transition temperature, which are listed in Table III. Similar to the decrease in storage modulus, a systematic decrease in tan δ is expected with increasing loading of tung oil methyl ester because the methyl ester reduces the crosslink density and subsequently increases the free volume and molecular motion and therefore decreasing the glass transition temperature.

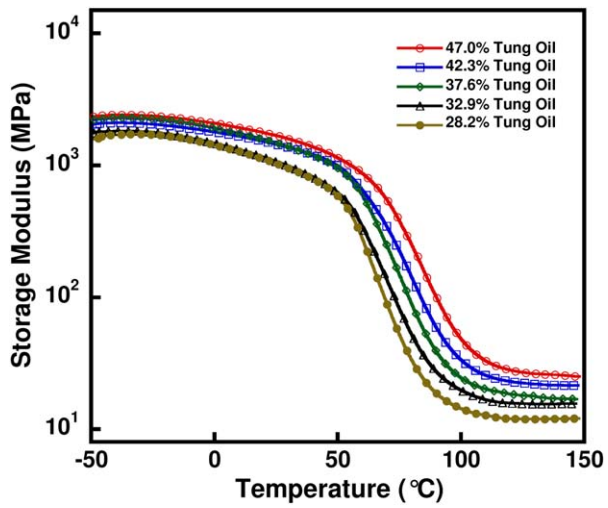

Figure 6. Variation in storage modulus as a function of tung oil and methyl ester concentrations. [Color figure can be viewed in the online issue, which is available at wileyonlinelibrary.com.]

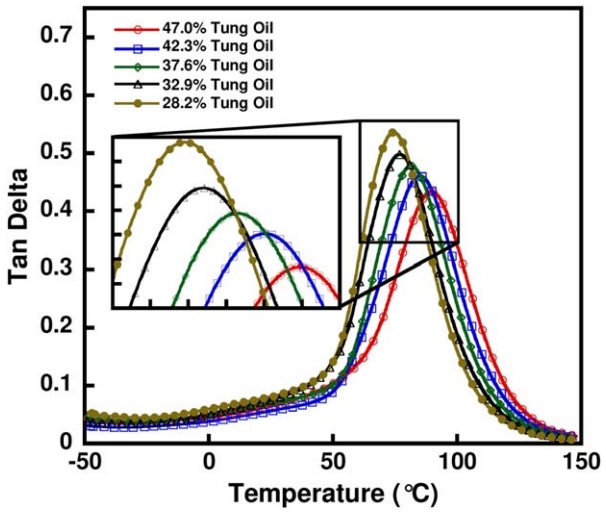

Figure 7. Variations in tan δ, or glass transition, as a function of tung oil and methyl ester concentrations. [Color figure can be viewed in the online issue, which is available at wileyonlinelibrary.com.]

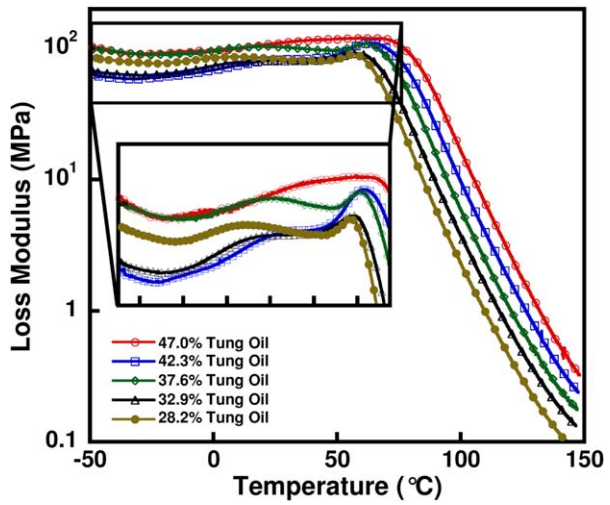

Figure 8. Variations in loss modulus as a function of tung oil and methyl ester concentrations. [Color figure can be viewed in the online issue, which is available at wileyonlinelibrary.com.]

The loss modulus, shown in Figure 8, indicates that phase separation took place. The 47.0% tung oil sample showed one single peak around the 80°C mark typical for a mostly homogenous polymer. However, as methyl ester was introduced to the formulation, a secondary peak formed, indication either phase separation or heterogeneous mixing. In addition, the pronouncement of the lower peak increased and shifted to lower temperatures with increasing methyl ester content. The reactivity of methyl ester was higher than that of tung oil triglyceride, therefore the methyl ester reacted earlier and created a softer phase in the polymer.

The higher reactivity of the methyl ester was corroborated through differential scanning calorimetry of the curing polymer seen in Figure 9. With increasing methyl ester content the heat flow curve formed an additional reaction peak at lower temperatures, indicating that tung oil methyl ester reacted faster than the other constituents in the thermoset. As the methyl ester content increases, the secondary reaction peak at the lower temperature also increases in size. It should also be noted that a shift of the dominant peak to higher temperature would typically indicate a slower reaction. However, in this case the shift is a result of the methyl ester quickly reacting with the catalyst first and causing it more difficult for the other constituents in the resin to come in contact with the catalyst. This preferential reaction with the methyl ester reinforces the concept of phase separation seen in the loss modulus of the samples with methyl ester.

Because the loss modulus curves indicated phase separation, transmission electron microscopy was used to investigate the

Table II. Molecular Weight Between Crosslinks

	47.0% Tung oil	42.3% Tung oil	37.6% Tung oil	32.9% Tung oil	28.2% Tung oil
M_C	0.47 Kg/mol	0.55 Kg/mol	0.67 Kg/mol	0.75 Kg/mol	0.97 Kg/mol

Table III. Glass Transition Temperature based on DMA Analysis

	47.0% Tung oil	42.3% Tung oil	37.6% Tung oil	32.9% Tung oil	28.2% Tung oil
T_g	89.7°C	85.1°C	81.1°C	76.8°C	74.5°C

microstructure of the thermosetting networks of 32.9% and 47.0% tung oil polymers. The TEM images in Figure 10, especially at the 10 nm scale, show phase separation in both samples investigated. The phase separation is shown as light and dark regions in the TEM images. Because styrene and divinylbenzene have high electron densities due to their phenolic rings, styrene and divinylbenzene rich phases are interpreted as the dark areas in the TEM images. Consequently, the lighter areas are from the triglyceride and methyl esters. The TEM images show phase separation s on the scale of three to five nanometers. At this small scale, the phases consist of only a few molecules, possibly bordering on a random coblock structure.

While using storage modulus to identify the crosslinking regularity, the molecules involved in the crosslinking are not identified. Soxhlet extraction identifies monomers that are incorporated into the thermoset network and the monomers that are not interconnected. The thermosets were washed with a refluxing solvent for 24 h in a Soxhlet extractor to remove the soluble portion of the polymer. The monomer components not incorporated into the network were dissolved in the solvent and then separated and identified by NMR. Figure 11 shows the NMR data from the soluble portion of the thermosets. As seen in the figure, the majority of the soluble portion is from various methyl esters. The first obvious methyl ester is the SoyGold used to homogenize the BFE when mixed. Because SoyGold has few double bonds and none are conjugated, the reactivity of SoyGold is low and therefore does not become incorporated into the thermosetting network. In addition, Tung oil fatty acids are

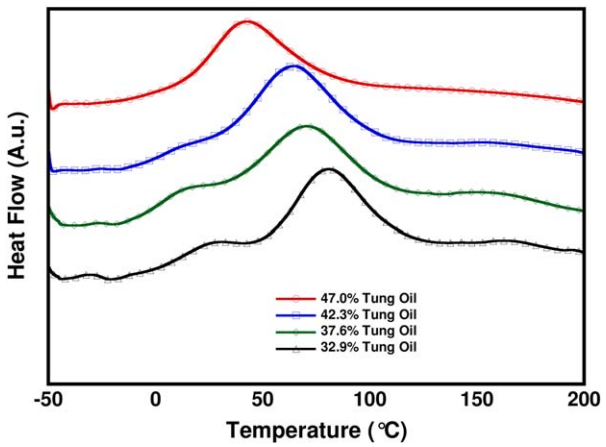

Figure 9. Curing of tung oil composites once mixed. Test run at a temperature rate of 3°C min^{-1}.Note: Samples of 28.2% tung oil were not tested because the reaction accelerated too fast to capture it. [Color figure can be viewed in the online issue, which is available at wileyonlinelibrary.com.]

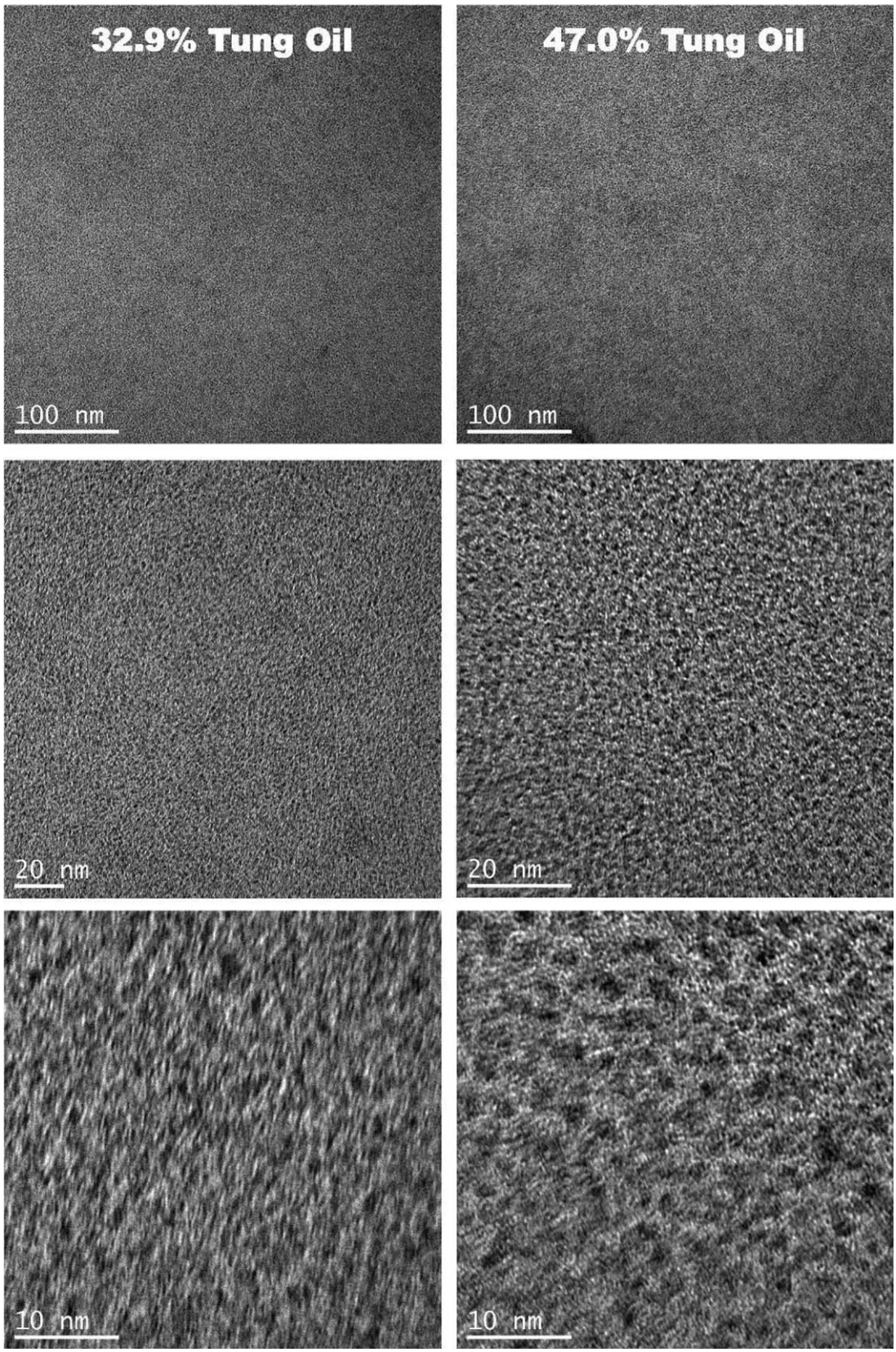

Figure 10. TEM of 32.9 and 47.0% tung oil polymers.

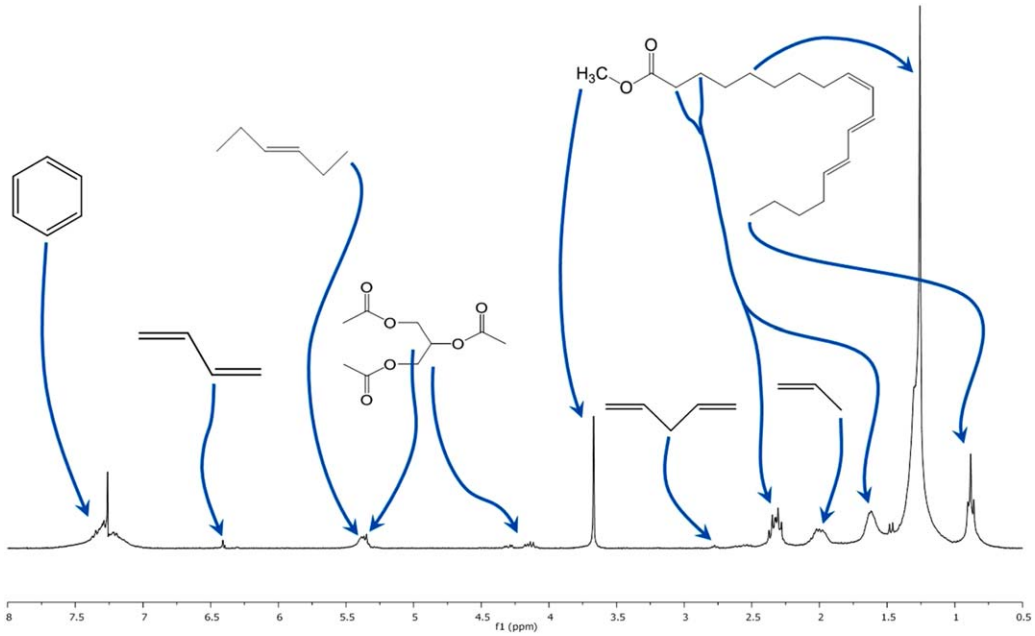

Figure 11. NMR of Soxhlet extraction. [Color figure can be viewed in the online issue, which is available at wileyonlinelibrary.com.]

Table IV. Weight Percentage of Soluble Thermoset Content

	47.0% Tung oil	42.3% Tung oil	37.6% Tung oil	32.9% Tung oil	28.2% Tung oil
wt %	3.3%	4.2%	5.2%	7.4%	9.5%

only 82% α-eleostearic acid, which is the fatty acid with three conjugated double bonds. The remaining mixture is of several other fatty acids—fatty acids with much less reactivity due to fewer double bonds and less conjugation. Because the esterification and saponification process cannot separate these fatty acids from the α-eleostearic acid, the tung oil methyl ester added to the reaction contains all the variations of methyl ester derived from the fatty acids including those that do not incorporate into the crosslinked network. The NMR shows that these methyl esters are not being incorporated. Peaks forming

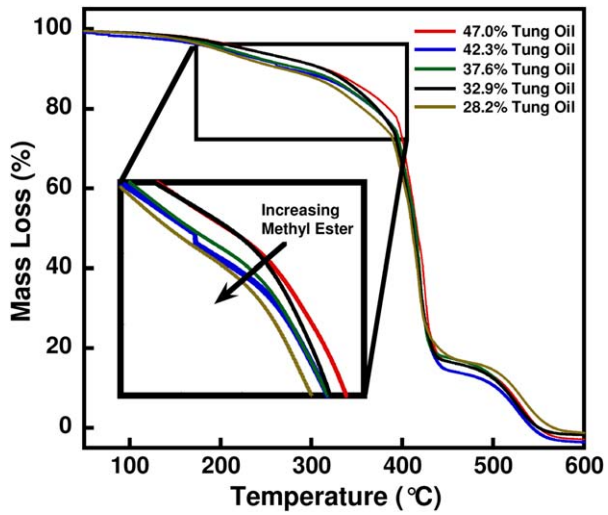

Figure 12. Variations in thermal stability as a function of tung oil and methyl ester concentrations using thermogravimetric analysis. [Color figure can be viewed in the online issue, which is available at wileyonlinelibrary.com.]

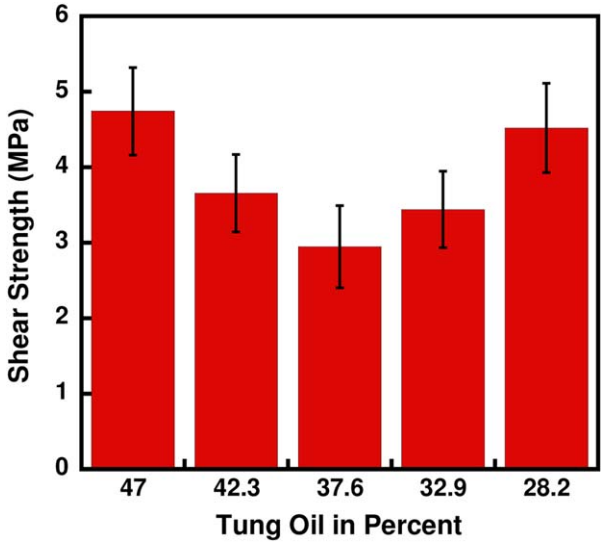

Figure 13. Compressive lap shear strength as a function of tung oil and methyl ester concentrations. [Color figure can be viewed in the online issue, which is available at wileyonlinelibrary.com.]

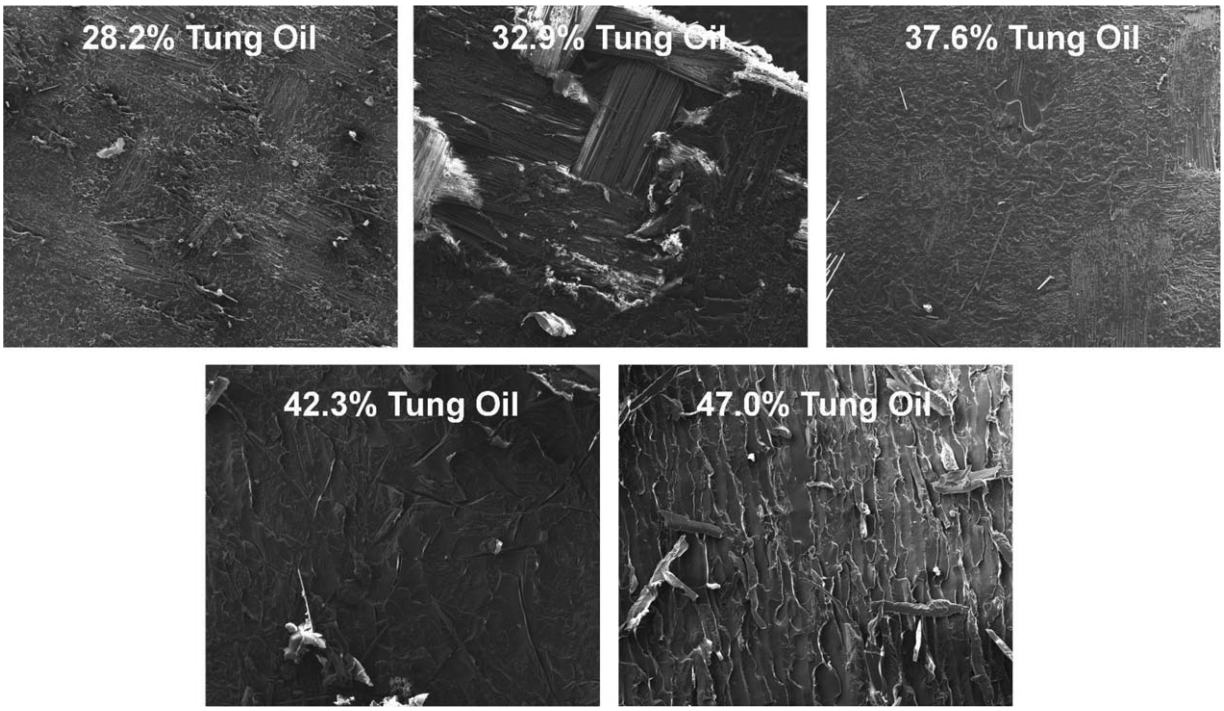

Figure 14. Lower magnification (×75) SEM images of crack surfaces.

in 0.5–4.0 show key resonance of general methyl esters. This peak range also contains the identifiers for the SoyGold methyl ester used as a solubility enhancer. Peaks above 4.0 show other minor components that do not incorporate such as the left over glycerin bond broken from the triglyceride during the saponification as well as benzene rings from a few styrene and divinylbenzene monomers that might not have tied into the network. Table IV shows the weight percentage of extractable components in the fully cured thermoset. While the soluble content increased with increasing methyl ester content, the majority of the tung oil methyl ester was incorporated into the network.

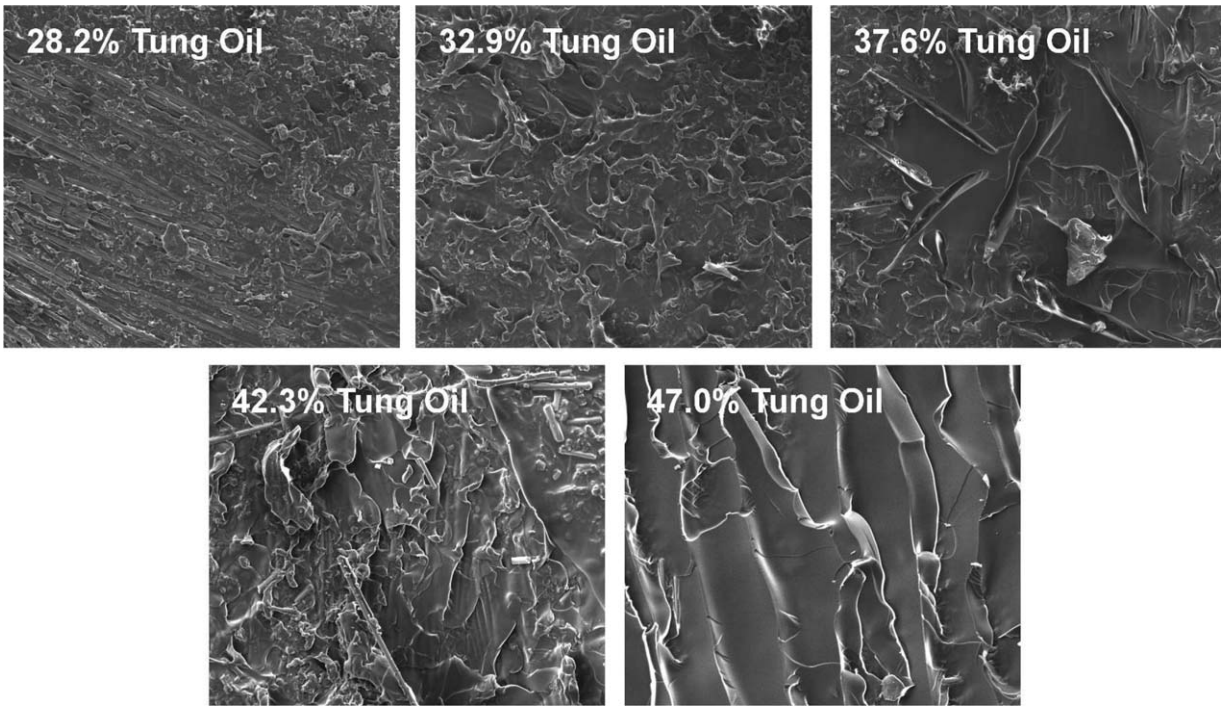

Figure 15. Higher magnification (×300) SEM images of crack surfaces.

Figure 12 shows the thermal stability of the thermosets. Thermogravimetric analysis showed that tung oil triglyceride underwent significant mass loss at ~275°C, while neat tung oil methyl ester exhibited significant mass loss at 175°C. Despite the large difference between thermal stability of methyl ester and triglyceride, the thermal stability of the thermosets did not show a significant reduction.

The thermosets underwent compressive lap shear testing according to ASTM D3846-08 to investigate their adhesive properties. Because these thermosets are to be used as a self-healing adhesive for bio-composites, the lap shear specimens were made from glass fiber biocomposites similar in composition to the bio-composites proposed for self-healing applications. The bio-composites were used solely as a substrate for which to apply the tung oil based thermosetting polymer. Figure 13 shows the lap shear strength values for tung oil-based thermoset samples.

Scanning electron microscopy of the sheared surfaces showed how the polymer fractured under compressive shear stress, see Figures 14 and 15. The SEM images revealed adhesive failure when the thermoset did not contain methyl ester. As the loading of methyl ester increased, the failure mode shifted to a cohesive failure as seen in the SEM images for 28.2 and 32.9% tung oil thermosets. In both cases fiber pullout can be clearly detected. In addition, SEM analysis showed that the thermosets transitioned from a brittle to a ductile failure mode. In thermosets without methyl ester components, the fracture surfaces showed brittle shearing, while increasing methyl ester content led to ductile failure of the thermosets. The fracture surfaces for the 42.3, 37.6, and 32.9% tung oil based thermosets showed signs of microcracks on the fracture surface. These microcracks formed in samples transitioning from brittle to ductile failures. The low shear stress value for 37.6% tung oil thermosets is likely caused by a combination of several factors—brittle to ductile transition, adhesive to cohesive failure transition, and microcracks. Figure 15 shows a higher magnification of the fracture surfaces to highlight the microcracks, fiber pullout, and ductile verse brittle failures.

CONCLUSION

Tung oil methyl ester can be utilized to modify the properties of tung oil based thermosetting polymers. This modification provides a uniform change in storage modulus and glass transition temperature, useful when tailoring to a specific application. In addition, methyl ester content increased the reactivity of the thermosets, which provided an added benefit because self-healing applications require rapid kinetic reactions. The thermal stability of the thermosets was not compromised by the addition of methyl ester.

While the addition of methyl ester caused a mixed shear stress response, all thermosets investigated provided more than adequate adhesive strength to cure microcracks. However, with an increase in methyl ester content, the thermosets exhibited cohesive failure, caused by the failure to maintain the bonds between fiber and matrix. Possible fiber treatments may improve the cohesive bonding of the polymer and consequently improve the shear strength properties.

For self-healing applications, thermosetting materials made from tung oil triglycerides, tung oil methyl esters, styrene, and divinylbenzene provided excellent material properties. Their mechanical properties and thermal stability identified them as structurally sound and stable candidates for crack healing. In addition, the low viscosity and fast kinetics provided for the required properties for flowing into a microcracks and solidifying in the crack plane. Once cured, these thermosets offer good adhesive properties, sustaining shear stresses exceeding 1 MPa. While in the past encapsulated self-healing work has been dominated by petroleum-based monomers, biorenewable materials, such as tung oil can provide the low viscosity, fast kinetics, mechanically sound, and thermally stable thermosets that can arrest microcracking.

REFERENCES

1. Osswald, T. A.; Menges, G. Materials Science of Polymers for Engineers; Hanser Gardner: Cincinnati, **2003**; p 16.
2. Chiellini, E.; Cinelli, P.; Corti, A. In Renewable Resources and Renewable Energy: A Global Challenge; Graziani, M., Fornasiero, P., Eds.; CRC Press: Boca Raton, FL, **2007**; p 63.
3. Bisio, A. L.; Xanthos, M. How to Manage Plastics Waste: Technology and Market Opportunities; Hanser Publishers: Munich, New York, **1995**.
4. Mustafa, M. Plastics Waste Management: Disposal, Recycling, Reuse; Marcel Dekker: New York, **1993**.
5. Johnson, L. A.; Myers, D. J. In Practical Handbook of Soybean Processing and Utilization; Erichson, D. R., Ed.; The American Oil Chemist's Society Press: Champaign, IL, **1995**; p 380–427.
6. Formo, M. W. In Bailey's Industrial Oil, Fat Products, Vol. *2*, 4th ed.; Swern, D., Ed.; Wiley: New York, **1982**; p 343.
7. Larock, R. C.; Li, F. Thermosetting Polymers from Cationic Copolymerization of Tung Oil: Synthesis and Characterization, *J. Appl. Polym. Sci.* **2000**, *78*, 1044.
8. Li, F.; Hanson, M. V.; Larock, R. C. *Polymer* **2001**, *42*, 1567.
9. Li, F.; Larock, R. C. *J. Polym. Environ.* **2002**, *10*, 59.
10. Li, F.; Hasjim, J.; Larock, R. C. *J. Appl. Polym. Sci.* **2003**, *90*, 1830.
11. Li, F.; Larock, R. C. *Biomacromolecules* **2003**, *4*, 1018.
12. Andjelkovic, D. D.; Lu, Y.; Kessler, M. R.; Larock, R. C. *Macromol. Mater. Eng.* **2009**, *294*, 472.
13. Mauldin, T. C.; Kessler, M. R. *Int. Mater. Rev.* **2010**, *55*, 317.
14. Li, F.; Larock, R. C. *J. Polym. Sci. B Polym. Phys.* **2000**, *38*, 2721.
15. Li, F.; Larock, R. C. *J. Polym. Sci. B Polym. Phys.* **2001**, *39*, 60.
16. Sheng, X.; Lee, J. K.; Kessler, M. R. *Polymer* **2009**, *50*, 1264.
17. Levita, G.; DePetris, S.; Marchetti, A.; Lazzeri, A. *J. Mater. Sci.*, **1991**, *26*, 2348.